

Research on a New Maximum Power Tracking Algorithm for Photovoltaic Power Generation Systems

Lei Shi^{1*}, Zongyu Zhang², Yongrui Yu³, Chun Xie⁴, and Tongbin Yang⁵

^{1,2,3,4,5}Guizhou Power Grid Co., Ltd. Intelligent Operation Center

Abstract

INTRODUCTION: Significant advances have been made in photovoltaic (PV) systems, resulting in the development of new Maximum Power Point Tracking (MPPT) methods. The output of PV systems is heavily influenced by the varying performance of solar-facing PV panels under different weather conditions. Partial shading (PS) conditions pose additional challenges, leading to multiple peaks in the power-voltage (P-V) curve and reduced output power. Therefore, controlling MPPT under partial shading conditions is a complex task.

OBJECTIVES: This study aims to introduce a novel MMPT algorithm based on the ant colony incorporated bald eagle search optimization (AC-BESO) method to enhance the efficiency of PV systems.

METHODS: The effectiveness of the proposed MPPT algorithm was established through a series of experiments using MATLAB software, tested under various levels of solar irradiance.

RESULTS: Compared to existing methods, the proposed AC-BESO algorithm stands out for its simplicity in implementation and reduced computational complexity. Furthermore, its tracking performance surpasses that of conventional methods, as validated through comparative analyses.

CONCLUSION: This study confirms the efficacy of the AC-BESO method over traditional strategies. It serves as a framework for selecting an MPPT approach when designing PV systems.

Keywords: PV systems; MPPT; Irradiation; Power output; Ant-colony integrated bald eagle search optimization (AC-BESO)

Received on 20 09 2024, accepted on 06 10 2024, published on 19 11 2024

Copyright © 2024 L. Shi *et al.*, licensed to EAI. This is an open access article distributed under the terms of the [CC BY-NC-SA 4.0](#), which permits copying, redistributing, remixing, transformation, and building upon the material in any medium so long as the original work is properly cited.

doi: 10.4108/ew.7325

1. Introduction

The depletion of natural fossil fuel supplies can be rapidly addressed by employing certain forms of renewable energy to meet the growing requirement for power. Renewable energy sources prove the capacity to generate electricity [1]. Solar energy is perhaps one of the most sustainable energy sources in the world given its availability and replenishment without necessarily polluting the environment and it can substitute for the production of electricity. The generation of solar energy is soaring higher each day. The increase in the reliability and convergence speed as a result of getting the most energy from harvesting are the reasons for this growth [2]. In addition, every

industry uses heating, electricity, etc. One estimate of the demand for renewable energy puts the figures for wind and solar energy at the promotion of renewable energy development [3].

To maximize the energy from the PV modules, several MPPT approaches have been developed over the past ten years. Still unclear, though, is how to choose a certain approach [4]. Sunlight incident on a solar cell (SC) generates DC power. To create a PV module, many SCs are linked. Eventually, the solar array is created by assembling the solar modules into groups. The nonlinear properties of the SCs cause PV elements to have comparatively poor transformation effectiveness. Utilizing the greatest power that the PV modules can produce, so it becomes essential [5].

* Corresponding author. Email: 15285646532@163.com

SCs generate direct current (DC) electricity when sunlight strikes them. A PV module is made up of several SCs associated with one another to generate more power [6][24-30]. A solar array can be made by combining these modules further. Nonetheless, the nonlinear properties of SCs place an occasionally tight restriction on the efficiency of the PV system. To optimize the quantity of energy that PV modules can create, it is imperative to enhance their power output (PO) [7]. Various circumstances in the atmospheric environment including sun direction, bird droppings, and array tilt angle PS from building structures and clouds make the intensity of light on the PV methods non-uniform. In addition, it may cause hotspots to appear as evidence of an extreme heat wave as a result of damaging the PV system. A PV system is connected in parallel with the bypass diode to minimize heat and power loss [8].

The most efficient operation guarantee of PV systems in a variety of climatic circumstances is the key rationale, where the MPPT algorithm exists based on complex mathematical models and control strategies [9]. The technology optimizes the amount of solar energy collected and enhances the overall efficiency and dependability of the photovoltaic approach by continuously determining the maximum power point tracking (MPPT) of the PV array. Further, to reduce the limiting effects of power loss and stress on the components the MPPT algorithm prolongs the PV system's life span. It is also important to note that system efficiency increases with the avoidance of superfluous heating while achieving better system reliability when a system is driven nearer to the MPP [10]. Therefore, this research aims at developing a new unique MPPT strategy called Ant-Colony Integrated Bald Eagle Search Optimization (AC-BESO) that will improve the effectiveness and dependability of PV systems.

Contribution of this paper

- This paper proposes a new MPPT algorithm known as AC-BESO MPPT algorithm to improve the performance of PV systems.
- The PS situations that lead to several points in the P-V curve and decreased power production are the specific issues that the suggested AC-BESO approach intends to overcome.
- Tracking efficiency is improved by the AC-BESO algorithm over traditional MPPT techniques.

Section 2 contains a list of related works. Section 3 presents the methodology. Section 4 is mentioned in the results. In section 5, the conclusion is provided.

2. Related works

Two approaches for reinforcement learning (RL) based on MPPT were presented in the investigation [11] through the Q-learning technique. Furthermore, of the two suggested techniques, the RL-Q-network (QN) MPPT approach produced maximum average energy, and the RL-Q-table (QT) MPPT approach performed with less oscillation.

The investigation subsequently builds a back propagation neural network (BPNN) based deep learning model [12] to get the MPP. The experiment demonstrated that the suggested approach obtains the optimum output energy from every panel contrasted to the traditional regression assessment techniques on the training, evaluation, and validating sets.

The investigation [13] presented the advanced memetic reinforcement learning (MRL) dependent MPPT approach for the PV systems, working in partial shadowing circumstances (PSC). However, when it compared to MRL with other traditional metaheuristic algorithms for MPPT of PSC, for example, MRL was much closer to the GMPP and their algorithm yields a better standard optimum. Consequently, a system could generate more power in different vagaries of a weather situation and seasons.

In the investigation [14] a proposed low-cost portable data logger for monitoring PV systems was developed, tested and analyzed. As indicated by the reported findings and derived features, the superiority of the suggested strategies in power generation prediction was validated.

The potential of using ML-based MPPT strategies for accomplishing the responsibility of power optimization in a PV system under a PSC scenario was discussed in the investigation [15]. The performance of the testing was revealed, indicating that the recommended ML-based algorithm, which was Weighted K-Nearest Neighbors (WK-NN) outperformed the remaining by a slight margin.

The ultra-short-term energy forecasting for the solar power manufacturing process was proven to have enhanced reliability with the use of an adaptive k-means (AK-M) and Gated Recurrent Unit (GRU) ML technique for short-term PV power forecast [16]. The comparison findings demonstrated the superiority, stability, and lower error rate of the suggested AK-M and GRU network model for immediate PV energy production forecast.

The purpose of the investigation [17] was to develop an ML data science innovative blended PV system power estimation for the building concerning its different facades. The findings showed that if a time and place were fixed, the model functions reliably and consistently with its functions. It could be ascertained that proper utilization of linear regression coefficients when employing the neural network might help to bring the forecasters to their maximum reliability.

The investigation aims to show [18] how an FNN controller could be used to depict an influential PV method with DC capability. The experimental results showed that, as compared to the conventional method, the proposed FNN controller based MPPT was higher at keeping the optimal values of power.

To provide an ML-based PV power generation projection in the short and long term, an effort was made by the investigation [19]. The work might be valuable to grid operators in selecting a suitable method for PV power prediction and scheduling the volatility of generation ahead of time.

A high-efficiency power point tracking technique was proposed in the investigation [20] to decrease power

oscillation and current ripple around the MPP. The fast variation of solar irradiation from 25% to 100% has been used to authorize the dependability and reliability of MPPT.

Regression controller (RC) based MPPT was established in the investigation [21] to attain maximum peak voltage under the PS effect. Perturb and Observe (P&O), Particle Swarm Optimization (PSO), and Flower Pollination Algorithm (FPA) algorithms were outperformed by the RC-based MPPT hardware and simulation outcomes where PV was PS by approximately 20%, 16.96%, and 15%, respectively.

An MPPT technique based on an irradiance estimate and a multi-kernel extreme learning machine (MKELM) was proposed in the investigation [22] to lower investment costs and increase the efficiency of PV systems. The recommended method's benefits over the conventional MPPT algorithm were confirmed through simulated studies conducted on the PV system in various operating circumstances.

The investigation [23] proposed a pulse width modulation (PWM) control boost converter in conjunction with an innovative support vector machine regression (SVMR) ML approach for solar panel MPPT. Despite fluctuating weather during the stable stage of operation of the solar PV system, the MPP tracking efficiency was more than 94% due to the SVM regression control approach.

The investigation [24] provided a scheduling method for hybrid solar and power management networks that relies on the proximal policy optimization (PPO) technique. These results showed that computing the time and generalization, the suggested deep reinforcement learning (DRL) based control strategy outperformed the conventional approaches.

The investigation [25] provided an overview of the MPPT technique for solar PV panels using a Deep Deterministic Policy Gradient (DDPG) agent of RL and a Digital Twin (DT). The overall power production improved by 10.45%, while simulations' settling time was 24.54 times faster.

3. Methodology

In PV infrastructure, the fast advancement of MPPT technology tackles issues caused by variable solar radiation and PS. To improve PV system performance, this work presents a novel MPPT algorithm called AC-BESO, which integrates bald eagle search with ant colony optimization. When compared to conventional techniques, experimental validation shows better tracking efficiency, providing a useful foundation for future PV system development.

3.1. PV array in PS situations

An array of PV modules is a network of several PV modules combined either in parallel or in series. Through a

series connection to increase the voltage intensity and a parallel interaction to increase the current stage, this configuration aims to increase the PV array's power capability. However, several variables, like surrounding construction, tree shades, cloud activity, and so forth, affect how evenly the series-connected PV modules get light. The uneven insolation on the panels results in PSC. Blocking and bypass diodes are employed to address these issues. In a PV structure, bypass diodes C_{Byp} are employed to decrease the adverse impacts of shade and shield the method from reverse bias circumstances-related damage. To ensure that other SCs continue to generate electricity and to prevent excessive power loss, they generate alternate pathways for current when an SC is covered. In contrast, blocking diodes C_{Block} are used, especially in off-grid networks with energy storage, to reset the solar panel's capacity or cease the battery's reversible current stream. This ensures effective energy transmission and safeguards the system's tools. The solar PV system's overall dependability and efficiency are enhanced by both kinds of diodes. This examination looks at a PV system that has three modules coupled in series. The P-V characteristics of these three components are under the assumption of irregular insolation. The non-uniform insolation results in three peaks. Two of these are local maxima, while one peak represents the global maximum. The performance of the overall string of series-associated PV modules is greatly impacted by the PS. Energy is lost when a shaded panel's effective voltage falls and frequently becomes negative due to reverse-biased conditions.

The distinction between local and global maxima is difficult for conventional MPPT algorithms to make since both points have zero slopes. Engineers have been using metaheuristic-based optimization strategies to solve this problem since they can search the whole space of solution vectors and find and utilize the maximum point. Population-based metaheuristic methods, including AC, have shown promise in solving this issue. Improved AC variations are introduced in the next section, to solve the energy monitoring issue in solar PV systems.

3.2. MPPT

The MPPT framework, shown in Figure 1, consists of a driving circuit, a DC-to-DC boost converter, a microcontroller, and a closed-loop controller combined with the aid of sensors. The computer determines the duty ratio value (DR_v), detects the PV array's voltage and current, and then uses the gate controller transistor to provide the tuned signal for the transformation. The controller uses the MPPT technique to find the optimal C_o

values from the PV array for ($O_{Max\ 0}$) extraction. Equation (1), which specifies the target variable (y) for the optimization procedure, is used to formulate the MPPT issue.

$$e(DR_{IJ}) = O_{Max\ 0} \tag{1}$$

In this work, the AC-BESO technique is utilized to determine the global MPP (GMPP), or maximum PO ($O_{Max\ 0}$) corresponding to the ideal value of (DR_{IJ}).

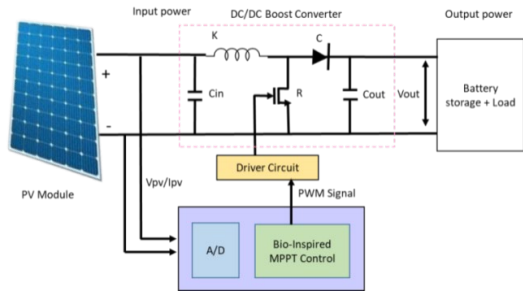


Figure 1. A typical PV system with MPPT control

3.3. Simulation of the PV System

A variant featuring just one diode is shown in Figure 2. Therefore, it consists of a unique current generator that is series impedance, shunt impedance, and anti-parallel to a single diode, to consider for ohmic losses and bleeding impedance to the bottom. Though it is more accurate and it can yield superior results, a two-diode model has certain drawbacks that make a problem harder. However, the single-diode model produces reasonable approximations and simplifies the modeling of PV cells. Consequently, a single-diode model is recommended for PV modeling. Multi-cell arrays coupled in series or parallel are commonly used to create PV modules. With the present generation, there are three modules associated with the series. The properties of the PV model depend on the temperature and solar radiation levels. Additionally influencing the properties of the single-diode model are the parallel conflicts and the series. The PV cell output current is denoted by the following formula (2) in mathematics.

$$J = J_o - J_{SAT} \left[\exp\left(\frac{r(U_p + J \cdot Q_{SE})}{b \cdot L \cdot S}\right) - 1 \right] - \frac{U_p + J \cdot Q_{SE}}{Q_{SH}} \tag{2}$$

Where J_{SAT} stands for the diode saturation current and J is the PV current. The diode current is shown by the J_o image the current flowing through the parallel resistor is called J_{SH} . R is the electronic charge symbol. U_p is the PV model's output voltage. Series resistance is known as Q_{SE} . Parallel impedance standards element Q_{SH} , is represented by m . L is Boltzmann's persistent S stands for the cell's temperature in degrees Celsius.

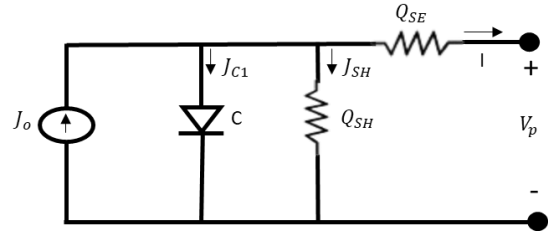


Figure 2. Analogous circuit of SCs

3.4. Characteristics of SCs

When an $SC_{I_{SC}}$ is linked in a short-circuit (Sh-C) configuration, the current that passes through it is known as Sh-C current. On the other hand, the maximum voltage that an SC can produce while there is no current flowing through it is V_{oc} known as the open-circuit voltage. It is imperative to realize that neither the open circuit nor the Sh-C phases effectively aid in the generation of energy. But there is a certain relationship between voltage and current that optimizes power production O_{max} . The performance of a PV cell at different levels of solar irradiation and constant temperature is depicted in Figures 3 and 4. PV power-voltage characteristics are shown in Figure 4, whereas current voltage characteristics are shown in Figure 3. These data indicate that while the Sh-C current of the PV cell maximizes significantly, the open-circuit voltage is only slightly affected by an increase in solar irradiation. Consequently, at constant temperature, the PV cell's power production is directly influenced by the amount of insolation.

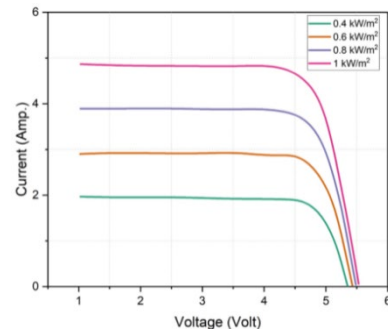


Figure 3. The effect of fluctuating Insolation on the current-voltage features of the SC

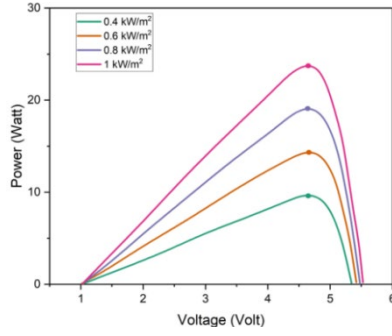


Figure 4. The effect of fluctuating Insolation quantities on the SC's power voltage properties

3.5. Ant-colony integrated bald eagle search optimization (AC-BESO)

It is intended to improve maximum power tracking in PV power generation devices. Maximizing the PO from solar panels and dynamically adapting to changing circumstances, improves efficiency.

3.5.1. ACO

A probabilistic approach called ant colony optimization (ACO) is used to determine the global optimal solution to a nonlinear issue. To optimize the path in a graph, ACO imitates the ants' foraging activity. A positive feedback phenomenon is created when several ants work together. At first, the ants arbitrarily search the path and leave behind pheromones for other ants to observe. The density of pheromone on a path increases with the number of ants that traverse it, increasing the probability that ants will follow identically and choose that path. Eventually, the majority of ants follow the route until individual ants use the sharing of such information to choose the quickest path. The ACO algorithm is first applied to combinational problems. More academics are using this technology in the constant domain these days, and their findings indicate that the ACO_Q performs better than other similar ACO algorithms. The process of creating solutions for continuous problems differs slightly from that of combinational problems. Assume that N parameters in a N -dimensional problem require optimization. The following is a description of the solution construction process.

First, L randomly generated solutions are created and kept in a solution archive of size ($L \geq M$). Subsequently, these L solutions are ordered based on the evaluation value in the minimization issue $e(t_1) \leq e(t_2) \leq \dots \leq e(t_k) \dots \leq e(t_L)$. This ranking is performed from greatest to poorest. The probability density variable for every dimension is a Gaussian function made up of several Gaussian sub-functions. This Gaussian kernel, which is provided, and

sampled for every dimension to produce the updated possibilities.

$$H_j(w) = \sum_{k=1}^L \omega_k h_k^j(w) = \sum_{k=1}^L \omega_k \frac{1}{\sigma_k^j \sqrt{2\pi}} \exp\left(-\frac{(w-\mu_k^j)^2}{2\sigma_k^{j2}}\right) \quad (3)$$

In this case, the j th element of the solution's Gaussian kernel is denoted by $H_j(w)$, the k th sub-Gaussian operates is denoted by $h_k^j(w)$, and the j th standard deviation and dimensional mean value are denoted by μ_k^j and σ_k^j , accordingly. The three Gaussian kernel parameters are determined using the following equations with L solutions in the repository.

Mean:

$$\mu^j = \{\mu_1^j, \dots, \mu_k^j, \dots, \mu_L^j\} = \{t_1^j, \dots, t_k^j, \dots, t_L^j\} \quad (4)$$

Where t_k^j denotes the k th solution's j th numerical component.

Standard deviation:

$$\sigma_k^j = \xi \sum_{i=1}^L \frac{|t_i^j - t_k^j|}{L-1} \quad (5)$$

Where the average distance between the selected response t_i and other responses in the preserve is multiplied by the parameter ξ indicating the speed of convergence to determine the standard deviation for the j th size of the k th approach.

Weight:

$$\omega_k = \frac{1}{QK\sqrt{2\pi}} \exp\left(-\frac{(k-1)^2}{2R^2L^2}\right), (\omega_L \leq \dots \leq \omega_k \leq \dots \leq \omega_2 \leq \omega_1) \quad (6)$$

Where R is the technique variable that denotes the significance of the top-ranked solutions, ω_k is the weight and k is the rank of the solution t_k . The probability of selecting the optimal ranking solution increases when R is small. There is an equal chance of selecting each response when it is enormous.

Two stages are involved in sampling a Gaussian kernel with numerous Gaussian sub-functions selecting the Gaussian function and then randomly sampling the selected Gaussian sub-function using the parameterized normal distribution. One can compute the possibility of selecting the k th Gaussian function employing.

$$o_1 = \frac{\omega_j}{\sum_{q=1}^L \omega_q} \quad (7)$$

For every new solution, the sampling procedure is repeated for every dimension ($j = 1, \dots, M$) until N , also known as the number of ants. Fresh approaches are developed. Following that, the initial solutions are supplemented with these N new ones. After ranking each of the $N + L$ responses once more, only the top L solutions are

retained in the archive. Consequently, the process is repeated in its entirety until either the higher amount of iterations is performed or the termination requirements are met. All of the ants will be successfully led to the optimal place in the search process by using this solution construction strategy.

A method for greedy search, dispersed computing, and positive feedback are combined in the ACO. It's quite good at finding the best solution. An early discovery of the ideal solution is ensured by the AC algorithm through the positive feedback mechanism. By avoiding premature integration distributed computing aids the ACO. The system's efficiency has improved since the greedy search finds an acceptable solution more quickly.

3.5.2. BESO

The BESO is a novel search optimization method inspired by the environment. It is a fish-hunting meta-heuristic algorithm that employs deceptive strategies. The BE uses devious social behavior to complete its three phases of ideal goal-achieving. Choosing the hunting area with the highest concentration of fish is the initial phase. The second phase is to search the hunting region. At this point, the eagle transfers into the area in search of fish by figuring out where the greatest place to search exists. Utilizing the finest categorizing position chosen in the second phase, the eagle chooses the optimal hunting spot in the third phase. It's the swooping phase right now. Swooping begins at the optimal hunting location and monitors entire subsequent actions toward it.

These are the phases of hunting that are taken into consideration.

I. Select phase

BEs choose the optimal fishing spot at this stage based on their prior awareness of food sources. As shown in (8), the novel hunting location selection, $O_{j,new}$ is indicated.

$$O_{j,new} = O_{best} + \alpha \times q(O_{mean} - O_j) \quad (8)$$

Where O_{best} denotes the ideal hunting position as determined by prior data. The regulating parameter α is assigned a value between 1.5 and 2. The random quantity q has a range of 0 to 1.28. O_{mean} , the mean position, is a reflection of all the data gathered from the earlier search regions. Eagles randomly examine all locations close to the previously chosen search spaces in the select stage for a new ideal hunting space.

II. Search phase

Eagles use circular motions in every direction inside the search area after choosing it. The eagle's updated posture to be prepared for a swoop is expressed as.

$$O_{j,new} = O_j + z(j) \times (O_j - O_{j+1}) + w(j) \times (O_{mean} - O_j) \quad (9)$$

Where $w(j)$ and $z(j)$ are given as.

$$w(j) = \frac{wq(j)}{\max(|wq|)}, z(j) = \frac{zq(j)}{\max(|zq|)} \quad (10)$$

$$wq(j) = q(j) \times \sin(\theta(j)), zq(j) = q(j) \times \cos(\theta(j)) \quad (11)$$

$$\theta(j) = b \times \pi \times rand \quad (12)$$

$$and \ q(j) = \theta(j) + Q \times rand \quad (13)$$

Equations 10–13 in a set describe Equation (9) uses spiral space as the form, the number of cycles and the movement's form are determined by the parameters b and Q there is a polar axis movement in the direction of the center point. While " Q " is between 0.5 and 2, b has a value between 5 and 10. The spiral path leading to the central point depicts the search space. The polar plots' moving point positions are between the range of 1 and 1.28. The ideal place to swoop is determined by comparison with the spiral space center location.

III. Swooping phase

Eagles move quickly in the direction of their prey after the optimal spot to swoop is identified. Eagles fly from the central point in the direction of their prey during this phase. The descriptions of 14–18 provide the updating of every point's position.

$$O_{j,new} = rand \times O_{best} + w1(j) \times (O_j - d1 \times O_{mean}) + z1(j) \times (O_j - d2 \times O_{best}) \quad (14)$$

Where

$$w1(j) = \frac{wq(j)}{\max(|wq|)}, z1(j) = \frac{zq(j)}{\max(|zq|)} \quad (15)$$

$$wq(j) = q(j) \times \sinh(\theta(j)), zq(j) = q(j) \times \cosh(\theta(j)) \quad (16)$$

$$\theta(j) = b \times \pi \times rand \quad (17)$$

$$and \ q(j) = \theta(j) \quad (18)$$

Where d_1 and d_2 are in the range.

3.6. Proposed technique

The combined AC-BESO technique, which incorporates the best aspects of both ACO and BESO, improves the performance and efficacy of the PV system MPPT. By using this method, PV systems' PO can be increased while simultaneously cumulative their general efficiency and dependability. The AC-BESO algorithm is especially

useful in situations where the environment is changing quickly, including temperature and sunshine fluctuations, where typical MPPT approaches might not be as effective. The combined AC-BESO algorithm is very effective for MPPT in dynamic and changing situations because it makes use of the strong exploratory characteristics of ACO and the fine-tuning specificity of BESO. Even in situations where partial shading is present, the hybrid algorithm increases the probability of locating the actual MPP by merging the ACO's broad search abilities with BESO's local refinement. The qualities of ACO and BESO are successfully combined in this combination approach, improving tracking precision, accelerating convergence, and producing robust performance all of which raise the overall efficiency and dependability of PV systems. Algorithm 1 shows the pseudo-code of Ant-colony integrated bald eagle search optimization (AC-BESO).

Table 1. Pseudo-code of Ant-colony integrated bald eagle search optimization (AC-BESO)

Algorithm 1: AC-BESO

```

% Initialize parameters
numAnts = 10; % Number of ants in the colony
numIterations = 100; % Number of iterations
pheromoneDecay = 0.5; % Pheromone decay rate
alpha = 1; % Pheromone influence factor
beta = 2; % Heuristic influence factor
Q = 1; % Pheromone update constant
bestSolution = []; % Initialize the best solution
bestFitness = Inf; % Initialize the best fitness value
% Initialize pheromone matrix and heuristic information matrix
pheromones = ones(nVariables); % Pheromone matrix
heuristicInfo = rand(nVariables); % Heuristic information matrix
% Initialize ant positions randomly
antPositions = rand(numAnts, nVariables);
% Main optimization loop
for iteration = 1: numIterations
% Evaluate fitness of each ant and update best solution
for ant = 1: numAnts
fitness =
evaluateFitness(antPositions(ant,:)); % Evaluate fitness of current ant
if fitness < bestFitness
bestFitness = fitness; % Update best fitness
bestSolution = antPositions(ant,:); % Update best solution
end
end
    
```

```

% update pheromone matrix
pheromones = (1 - pheromoneDecay) *
pheromones; % Decay pheromones
for ant = 1: numAnts
deltaPheromones = Q /
evaluateFitness(antPositions(ant,:)); % Pheromone update for current ant
pheromones = pheromones + deltaPheromones;
% Update pheromones
end
% Update ant positions using AC
- BESO algorithm
for ant = 1: numAnts
probabilities = (pheromones.^alpha) .*
(heuristicInfo.^beta); % Compute probabilities
antPositions(ant,:) = rand(1, nVariables) <
probabilities; % Update ant positions
end
end
% Final best solution and fitness
disp('Best Solution:');
disp(bestSolution);
disp('Best Fitness:');
disp(bestFitness);
% Fitness evaluation function
function fitness = evaluateFitness(solution)
% Example fitness function
fitness = sum(solution); % Fitness is the sum of solution elements
end
    
```

4. Result

In this section, we show the simulation model in detail and carry out a systematic examination. We have created a PV system in MATLAB to assess the efficacy of the AC-BESO-based MPPT technique. Table 2 provides a comprehensive overview of the PV component attributes in the experiments.

Table 2. Description of PV modules

Parameter	Value
Amount of PV panels connected in series	3
Short – circuit Current (I_{sc})	6.00 A
PV cells per module	60
Open – circuit Voltage (V_{oc})	22.50 V

Current at MPP (I_{Mp})	5.70 A
Voltage at MPP (V_{Mp})	18.00 V
Maximum Power (O_{Mp})	102.60 W
Temperature Coefficient of U_{oc} (%/ $^{\circ}C$)	-0.33
Temperature Coefficient of J_{sc} (%/ $^{\circ}C$)	0.04

4.1. Circumstances for Constant PS

Simulation tests employing varying degrees of solar Insolation (radiation) were conducted to compare the efficacy of the AC-BESO-based MPPT methodology with existing AC and AC- variable-coefficient (VC) systems.

4.1.1. Circumstance 1: Full Insolation

The PO and duty ratio graphs for a three-component PV array functioning through complete insolation circumstances are shown in the simulation outcomes that are provided in Figure 5a–c. For analysis, three distinct algorithms AC, AC-VC, and AC-BESO were used. Under these circumstances, a constant 1000 watts per square meter (W/m^2) of irradiance was applied to each PV module. The results show that in contrast to the AC and AC-VC methods, AC-BESO performed better in regard to tracking time and less fluctuations. With a tracking effectiveness of 99.96%, AC-BESO effectively monitored the MPP at 88.21 W, obtaining a convergence time of 0.36 seconds (s). Conversely, AC-VC, which had a settling time of only 1.3s, was able to follow the MPP more quickly than AC-BESO. AC-VC acquired a partially minimized MPP rate of 87.6 W with an effectiveness of 99.28%. Conversely, the MPP at 86.07 W is successfully tracked by the AC algorithm, which is renowned for its exploring and exploiting capabilities. However, it requires 1.36s to settle, which is longer than AC-BESO and AC-VC. Moreover, constant-state oscillations because of power damages and a 97.59% decrease in the MPP's performance, however, AC still performs better even in these situations. Although AC-BESO performs better in fully isolated environments, it is important to highlight that metaheuristic algorithms can also handle PS scenarios. Apart from demonstrating ideal performance, these algorithms must also be resilient and flexible enough to handle situations in which the PV array may be partially shaded.

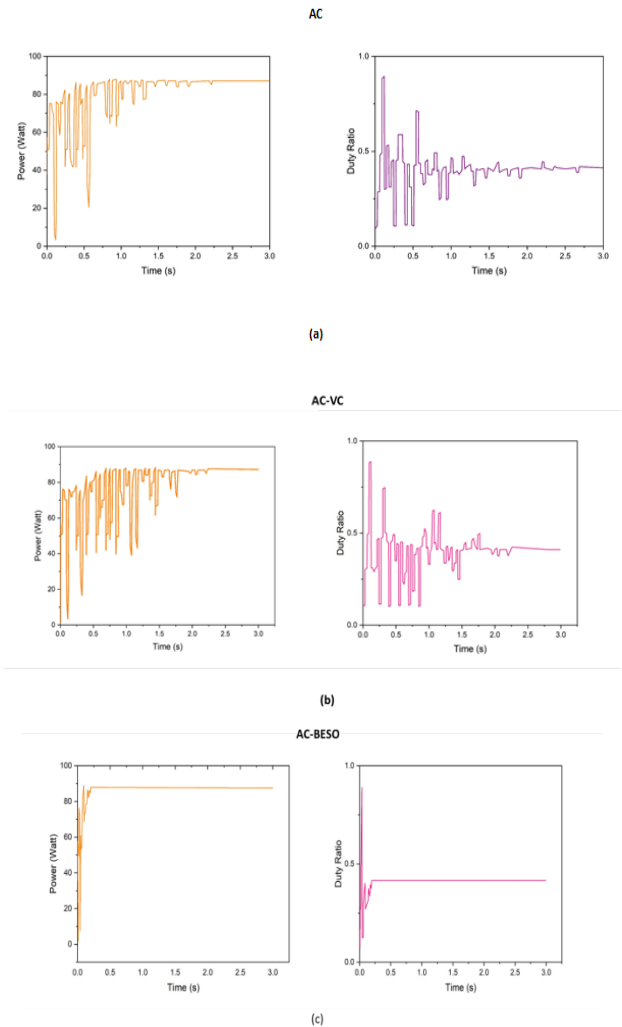


Figure 5. (a–c) Experimental outcomes of AC, AC-VC, and AC-BESO algorithm at Circumstance 1

4.1.2. Circumstance 2: Insufficient PS circumstance

Comparing findings for AC, AC-VC, and AC-BESO during circumstance 2, where PV array components endure various insolation levels of 1000, 900, 600, and 400 W/m^2 , are shown in Figures 6a, b, and c, accordingly. In this case, AC-BESO tracks the MPP at 42.27 W effectively in 0.499s of settling duration, resulting in an effectiveness of about 99.98%. With a settling duration of 1.28s, AC-VC has an effectiveness of 99.78% and a lower MPP rating of 42.16 W. In contrast, AC monitors the MPP of 42.05 W with achievement, but the effectiveness is only 99.51%, which is less than that of AC-BESO and AC-VC. Additionally, AC shows a longer settling duration of 1.341s. Particularly, AC-BESO performed significantly better in terms of settling duration than the other two techniques. The outcomes also reveal that the AC-BESO method performs significantly faster at convergent states than the AC and AC-VC algorithms, and more effective overall.

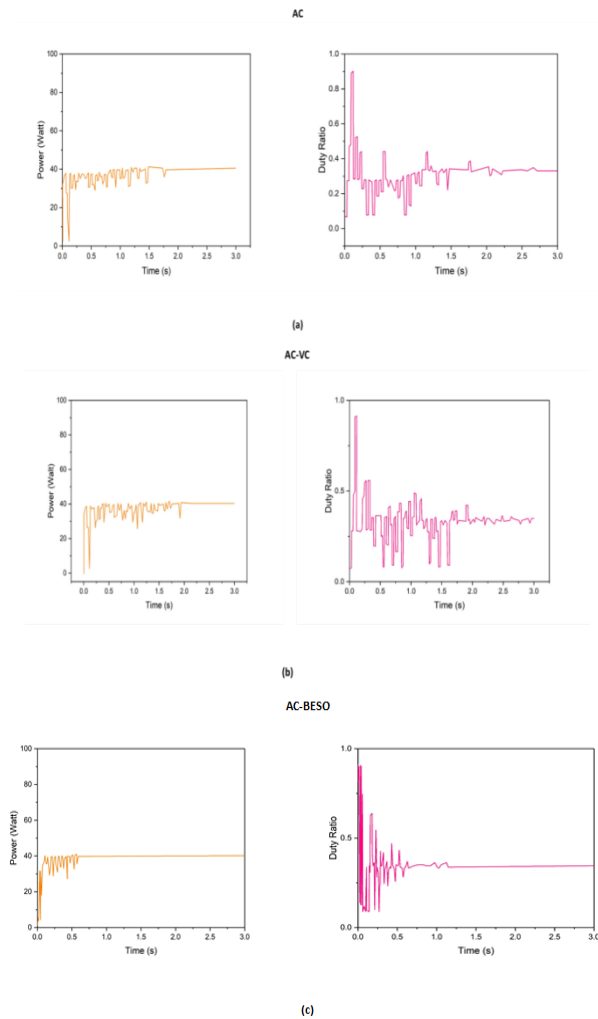


Figure 6. (a–c) Experimental outcomes of AC, AC-VC, and AC-BESO algorithm at Circumstance 2

4.1.3. Circumstance 3: significant PS circumstance

Figure 7a–c is used to contrast the outcomes for circumstance 3, where the single panel is assigned 1000 W/m², while the other panels are assigned 800 W/m², 750 W/m², and 500 W/m², accordingly. With a settling duration of 0.6014s and an effectiveness of almost 99.94%, AC-BESO follows the MPP at 49.73W with efficiency under this significant PS situation. Conversely, AC-VC resolves at 49.39W with 99.33% effectiveness, a considerably lower figure, after a longer monitoring period of 2.159s. When contrasted with other techniques, AC monitors the MPP of 49.25W with a tracking duration of 2.298s and a lesser effectiveness of 98.97%. When contrasted with AC-VC and AC, AC-BESO shows fewer variations throughout the MPP search, which results in a notable decrease in power losses. Figure 8 provides a concise comparative summary of all AC-BESO, AC-VC, and AC techniques, converging on their MPP tracking capabilities, efficiency, and tracking time.

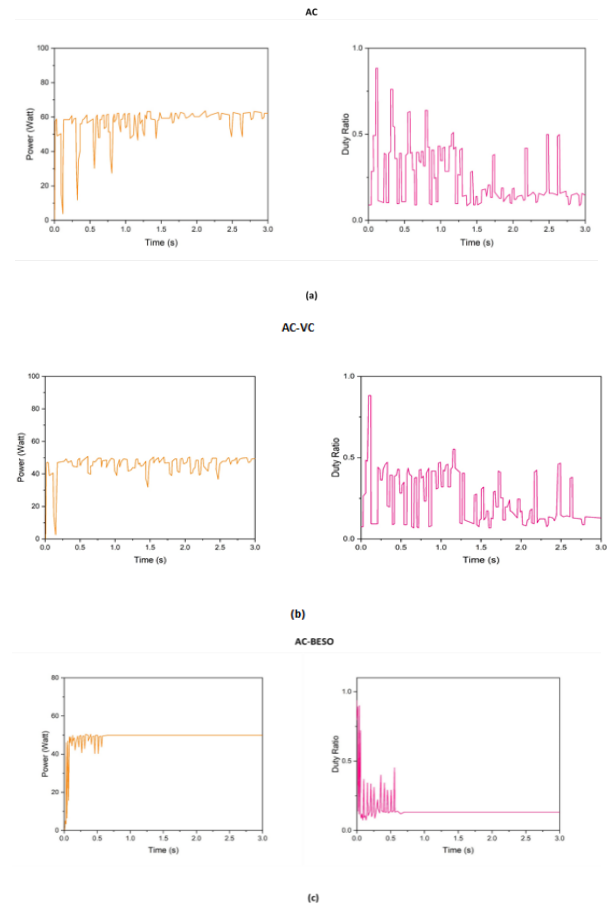
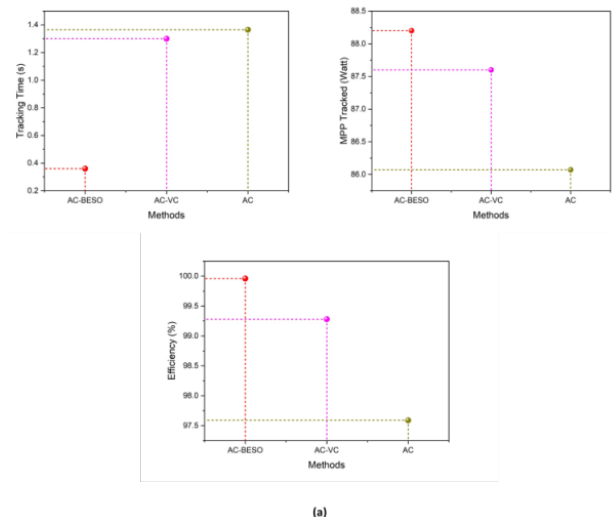


Figure 7. (a–c) Experimental outcomes of AC, AC-VC, and AC-BESO algorithm at Circumstance 1



(a)

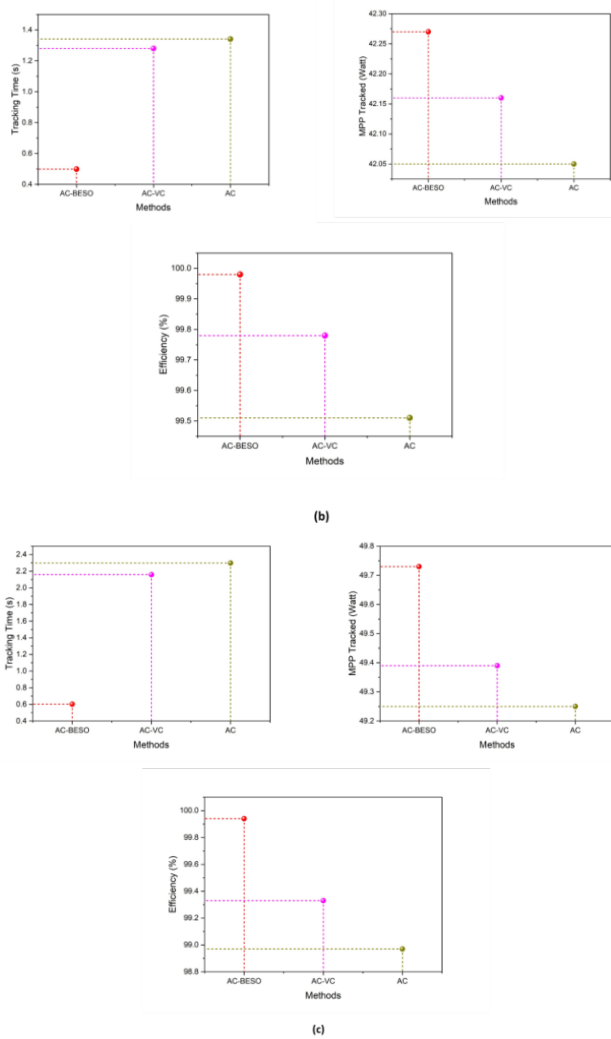


Figure 8. (a–c) Experimental outcomes of AC, AC-VC, and AC-BESO algorithm for efficiency, MPP tracked, and tracking time of Circumstances 1, 2, and 3.

4.2 Dynamic PS circumstance

To enhance the supremacy, adaptability, dependability, and effectiveness of the AC-BESO-based MPPT technique, its efficacy is assessed in the situation of dynamic variations in insolation circumstances. Considering environmental variations lead PV arrays to suffer varying degrees of shade in real-world circumstances, testing under dynamic circumstances is crucial. Consequently, a progressive variation in insolation is included in this experiment. Figure 9 shows sudden variations in incidence insolation values on the PV array. After a second, the original uniform distribution from circumstance 1 is changed to a mild PS scenario with insolation levels of 1000 W/m², 900 W/m², 600 W/m², and 400 W/m². After that, this is changed even

more to a PS circumstance with an insolation value of 900 W/m², 800 W/m², 500 W/m², and 400 W/m², much similar to circumstance 3. Finally, the fourth insolation level 1000W/m², 800W/m², 500W/m², and 300W/m² after 1s takes the place of the third insolation stage. The insolation phase varies at intervals of one second. To track the MPP rapidly, the algorithm has to repeat itself in reaction to these variations in insolation AC-BESO intersections in 0.4s and generates a higher power of 86.1W at a constant insolation degree, resulting in an effectiveness of 99.69%. The insolation stages of the PV array quickly change from stage 1 to stage 2. With a productivity of 99.93%, AC-BESO monitored an MPP of 39.32W in 1.33s at this insolation stage. It takes 2.182s to monitor the MPP of 39.52W at the third insolation stage. It took 3.27s to identify the MPP of 37.99W at the final insolation stage. The simulation results show that the proposed AC-BESO method is quite complicated due to variations in shaded configurations. The findings also suggest that the suggested AC-BESO might effectively imitate GMPP in the short term and show fewer oscillations in the fluctuations.

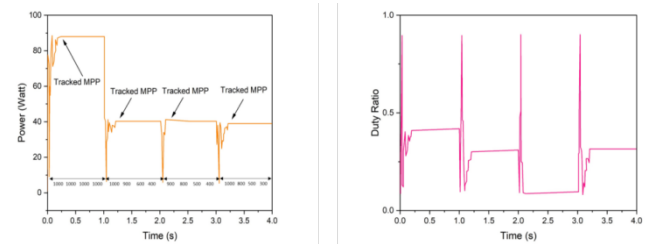


Figure 9. AC-BESO-based MPPT experiment outcomes for dynamic insolation circumstances

4.3. Impact of Load Variation

The experimental findings in this part show how the suggested AC-BESO-based MPPT approach is resilient and reliable even under varying loads. This fluctuation is shown on the three PV array components in Figure 10 with constant irradiances of 1000, 900, 750, and 400 W/m². A 15° load is delivered initially, then after 1s, the load changes to a 10° load. The findings show that the greatest power monitored in 0.33s with a 15Ω load is 49.98W. The highest power measured reaches 49.94W during a 0.18s period after the load shifts to 10Ω.

As a result, the maximum power tracked varies only slightly when the load is changed. These discrepancies are assigned to duration increases in monitoring as well as modifications in the magnitude and occurrence of energy oscillations through the initial repetitions. However, these differences are small and do not lead to large power losses.

For this reason, even when the load is changed, the suggested algorithm performs steadily.

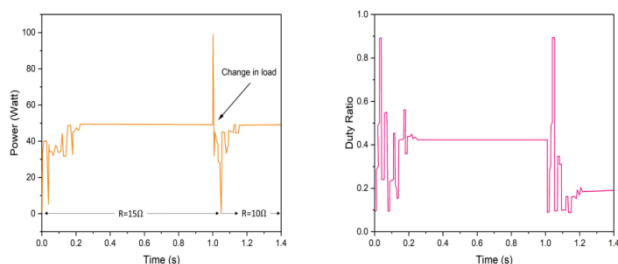


Figure 10. The results of an MPPT experiment using AC-BESO with varying loads between 10 and 15 Ω

4.4. Impact of PV Module Variation

The PV module, which is sold commercially, is used in this subsection to validate the suggested AC-BESO-based MPPT approach using the MATLAB R2020a software platform. The AC-BESO technique's MPP tracking capabilities are demonstrated in Figure 11, which displays the curves that match to the data.

Figure 11 shows the PV output curve to thoroughly assess the practicality of the proposed method when the exposure circumstance transitions from circumstance 1 (1000,1000,1000,600 W/m^2) to circumstance 2 (1000,900,700,600 W/m^2) during a 1-s time. In this case, the algorithm's reliability is highlighted by the fact that both monitoring duration and system performance are undisturbed.

After thoroughly evaluating various module results, shading conditions, and varying irradiance, the proposed algorithm demonstrates exceptional protection and flexibility. circumstances although it is essential to acknowledge that there is no absolute promise of the highest efficiency of any method in all settings. Its reliability for industrial operations is reinforced by its constancy. Specifically, the algorithm's ability to function well with varying module configurations suggests that it can be useful for changing the array's score. For example, if an array's scoring is changed, the current MPP tracker that has the AC-BESO algorithm installed and kept, preventing expenditure on buying a new tracker. Furthermore, the robustness of the tracker after a change in module scoring implies that it will continue to provide reliable efficiency for years to come, negating the need for replacement when a modern PV array is deployed.

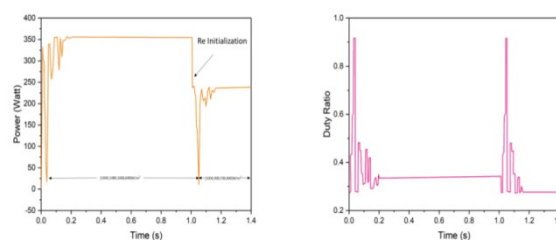


Figure 11. when circumstances 1 and 2 are dynamically switched in terms of incidence.

The proposed method is evaluated in terms of Average Efficiency (%), Tracking Time (sec), and Oscillations around the GMPP and compared with the existing approaches, which are Radial Basis Neural Network (RBNN), Perturb and Observe (P & O) and Incremental Conductance (InC) [26]. Table 2 shows the overall performance.

Our suggested AC-BESO approach performed a Tracking Time (Sec) of 0.26s, Oscillations around the GMPP(zero), and Average Efficiency of 96.6 % in contrast to the traditional techniques such as RBNN, P & O, and InC. The outcomes demonstrate that the suggested strategy outperforms existing methods.

Table 3. Overall performance

MPPT approach	Total Performance Indices	PS Circumstance
RBNN	Tracking Time (Sec)	0.028
	Oscillations around the GMPP	Zero
	Average Efficiency (%)	95.6466
P & O	Tracking Time (Sec)	0.25
	Oscillations around the GMPP	Very High
	Average Efficiency (%)	79.6566
InC	Tracking Time (Sec)	0.308
	Oscillations around the GMPP	Very High

	Average Efficiency (%)	81.006
AC-BESO [proposed]	Tracking Time (Sec)	0.26
	Oscillations around the GMPP	High
	Average Efficiency (%)	96.6

5. Conclusion

This investigation developed a new MPPT technique that integrates AC-BESO to increase the performance of the PV method. The recommended technique was employed to solve more critical PSC challenges that tend to result in more slopes in the P-V curve and lower voltages. The AC-BESO technique outperformed the traditional MPPT approaches in terms of effectiveness (96.6%) utilizing massive Matlab experiments for various solar energy stages. The outcomes indicate that the AC-BESO method could be applied to PV methods by efficiently conserving the optimal PO even in severe weather circumstances. Constraints include the ability of large-scale PV systems to scale, withstand environmental variations, adapt to varying energy demands, and accomplish effective assembly in a timely manner. Furthermore, the improvement of AI-driven search and the use of predictive analytics can be redirected into a dependable and effective PV power generation system.

References

- [1] He, B., & Bhatti, U. A. (2024). Smart Cities and Smart Networks: AI Applications in Urban Geography and Industrial Communication. *International Journal of High Speed Electronics and Systems*, 2440122.
- [2] Tang, H., Zhang, Z., Zhang, Y., Xu, B., & Bhatti, U. A. (2024, June). Plug-and-Work edge collaborator design for customised manufacturing. In *2024 39th Youth Academic Annual Conference of Chinese Association of Automation (YAC)* (pp. 63-68). IEEE.
- [3] Tang, H., Chen, D., Zhang, Y., Xu, B., Bhatti, U. A., & Yu, M. (2024, June). Bidirectional Interaction Techniques Based on Device Digital Twin Model. In *2024 39th Youth Academic Annual Conference of Chinese Association of Automation (YAC)* (pp. 132-138). IEEE.
- [4] Didi, F., Chaouche, M.S., Amari, M., Guezmir, A., Belhenniche, K. and Chellali, A., 2023. Design and Simulation of Grid-Connected Photovoltaic System's Performance Analysis with Optimal Control of Maximum Power Point Tracking MPPT Based on Artificial Intelligence. *Tobacco Regulatory Science (TRS)*, pp.1074-1098.
- [5] Hai, T., Zain, J.M. and Nakamura, H., 2023. Maximum power point tracking technique based on variable step size with sliding mode controller in photovoltaic system. *Soft Computing*, 27(7), pp.3829-3845.
- [6] Azam, M.S., Bhattacharjee, A., Hassan, M., Rahaman, M., Aziz, S., Shaikh, M.A.A. and Islam, M.S., 2024. Performance enhancement of solar PV system introducing semi-continuous tracking algorithm based solar tracker. *Energy*, 289, p.129989.
- [7] Guanghua, L., Siddiqui, F.A., Aman, M.M., Shah, S.H.H., Ali, A., Soomar, A.M. and Shaikh, S., 2024. Improved maximum power point tracking algorithms by using numerical analysis techniques for photovoltaic systems. *Results in Engineering*, 21, p.101740.
- [8] Ahmed, S., Mekhilef, S., Mubin, M.B. and Tey, K.S., 2022. Performances of the adaptive conventional maximum power point tracking algorithms for solar photovoltaic system. *Sustainable Energy Technologies and Assessments*, 53, p.102390.
- [9] Xu, S., Gao, Y., Zhou, G. and Mao, G., 2020. A global maximum power point tracking algorithm for photovoltaic systems under partially shaded conditions using modified maximum power trapezium method. *IEEE Transactions on industrial electronics*, 68(1), pp.370-380.
- [10] Verma, P., Alam, A., Sarwar, A., Tariq, M., Vahedi, H., Gupta, D., Ahmad, S. and Shah Noor Mohamed, A., 2021. Meta-heuristic optimization techniques used for maximum power point tracking in solar pv system. *Electronics*, 10(19), p.2419.
- [11] Chou, K.Y., Yang, S.T. and Chen, Y.P., 2019. Maximum power point tracking of photovoltaic system based on reinforcement learning. *Sensors*, 19(22), p.5054.
- [12] Rafeeq Ahmed, K., Sayeed, F., Logavani, K., Catherine, T.J., Ralhan, S., Singh, M., Prabu, R.T., Subramanian, B.B. and Kassa, A., 2022. Maximum power point tracking of PV grids using deep learning. *International Journal of Photoenergy*, 2022(1), p.1123251.
- [13] Zhang, X., Li, S., He, T., Yang, B., Yu, T., Li, H., Jiang, L. and Sun, L., 2019. Memetic reinforcement learning based maximum power point tracking design for PV systems under partial shading condition. *Energy*, 174, pp.1079-1090.
- [14] Patel, A., Swathika, O.G., Subramaniam, U., Babu, T.S., Tripathi, A., Nag, S., Karthick, A. and Muhibbullah, M., 2022. A practical approach for predicting power in a small-scale off-grid photovoltaic system using machine learning algorithms. *International Journal of Photoenergy*, 2022(1), p.9194537.
- [15] Nkambule, M.S., Hasan, A.N., Ali, A., Hong, J. and Geem, Z.W., 2021. Comprehensive evaluation of machine learning MPPT algorithms for a PV system under different weather conditions. *Journal of Electrical Engineering & Technology*, 16, pp.411-427.
- [16] Liu, Y., 2022. Short-Term Prediction Method of Solar Photovoltaic Power Generation Based on Machine Learning in Smart Grid. *Mathematical Problems in Engineering*, 2022(1), p.8478790.
- [17] Kabilan, R., Chandran, V., Yogapriya, J., Karthick, A., Gandhi, P.P., Mohanavel, V., Rahim, R. and Manoharan, S., 2021. Short-Term Power Prediction of Building Integrated Photovoltaic (BIPV) System Based on Machine Learning Algorithms. *International Journal of Photoenergy*, 2021(1), p.5582418.
- [18] Hameed, W.I., Saleh, A.L., Sawadi, B.A., Al-Yasir, Y.I. and Abd-Alhameed, R.A., 2019. Maximum power point tracking for photovoltaic system by using fuzzy neural network. *Inventions*, 4(3), p.33.
- [19] Mahmud, K., Azam, S., Karim, A., Zobaed, S., Shanmugam, B. and Mathur, D., 2021. Machine learning

- based PV power generation forecasting in Alice Springs. *IEEE Access*, 9, pp.46117-46128.
- [20] Abokhalil, A., 2020. Maximum power point tracking for a PV system using tuned support vector regression by particle swarm optimization. *Journal of Engineering Research*, 8(4).
- [21] Padmavathi, N., Chilambuchelvan, A. and Shanker, N.R., 2021. Maximum power point tracking during partial shading effect in PV system using machine learning regression controller. *Journal of Electrical Engineering & Technology*, 16, pp.737-748.
- [22] Xie, Z. and Wu, Z., 2021. Maximum power point tracking algorithm of PV system based on irradiance estimation and multi-kernel extreme learning machine. *Sustainable Energy Technologies and Assessments*, 44, p.101090.
- [23] Mahesh, P.V., Meyyappan, S. and Alla, R., 2023. Support Vector Regression Machine Learning based Maximum Power Point Tracking for Solar Photovoltaic systems. *International Journal of Electrical and Computer Engineering Systems*, 14(1), pp.100-108.
- [24] Guo, M., Ren, M., Chen, J., Cheng, L. and Yang, Z., 2023. Tracking Photovoltaic Power Output Schedule of the Energy Storage System Based on Reinforcement Learning. *Energies*, 16(15), p.5840.
- [25] Artetxe, E., Uralde, J., Barambones, O., Calvo, I. and Martin, I., 2023. Maximum Power Point Tracker Controller for Solar Photovoltaic Based on Reinforcement Learning Agent with a Digital Twin. *Mathematics*, 11(9), p.2166.
- [26] Bollipo, R.B., Mikkili, S. and Bonthagorla, P.K., 2023. Application of radial basis neural network in MPPT technique for stand-alone PV system under partial shading conditions. *IETE Journal of Research*, 69(9), pp.6409-6430.
- [27] Bristi, S. D., Tatha, M. J., Ali, M. F., Bhatti, U. A., Sarker, S. K., Masud, M., ... & Saha, D. K. (2023). A Meta-Heuristic Sustainable Intelligent Internet of Things Framework for Bearing Fault Diagnosis of Electric Motor under Variable Load Conditions. *Sustainability*, 15(24), 16722.
- [28] Ali, A., Li, J., Chen, H., Bhatti, U. A., & Khan, A. (2023). Real-Time Spammers Detection Based on Metadata Features with Machine Learning. *Intelligent Automation & Soft Computing*, 38(3).
- [29] Cheng, M., Li, D., Zhou, N., Tang, H., Wang, G., Li, S., ... & Khan, M. K. (2023). Vision-motion codesign for low-level trajectory generation in visual servoing systems. *IEEE Transactions on Instrumentation and Measurement*.
- [30] Chen, H., Zhang, Y., Bhatti, U. A., & Huang, M. (2023). Safe decision controller for autonomous driving based on deep reinforcement learning in non-deterministic environment. *Sensors*, 23(3), 1198.